Localizing Hydrological Drought Early Warning using In-Situ Groundwater Sensors

W. A. Veness[1,2*], A. P. Butler[1], B. F. Ochoa-Tocachi[1,2], S. Moulds[1] & W. Buytaert[1,2]

[1] Department of Civil and Environmental Engineering, Imperial College London, London SW7 2AZ, UK

[2] Grantham Institute – Climate Change and the Environment, Imperial College London, London SW7 2AZ, UK

*Corresponding author: William Veness (william.veness13@imperial.ac.uk)

Key Points:

- Advancements in sensing technologies give renewed feasibility to in-situ groundwater monitoring in data-scarce, drought-prone countries.
- Calibrating groundwater models with short observation records (weeks) substantially improves on satellite-based drought exposure indicators.
- Improved water availability assessment with in-situ sensors provides opportunities for better drought early warning and risk-mitigation.

Abstract

Drought Early Warning Systems (DEWSs) aim to spatially monitor and forecast risk of water shortage to inform early, risk-mitigating interventions. However, due to the scarcity of in-situ monitoring in groundwater-dependent arid zones, spatial drought exposure is inferred using maps of satellite-based indicators such as rainfall anomalies, soil moisture and vegetation indices. On the local scale, these coarse-resolution proxy indicators provide a poor inference of groundwater availability. The improving affordability and technical capability of modern sensors significantly increases the feasibility of taking direct groundwater level measurements in data-scarce, arid regions on a larger scale. Here, we assess the potential of in-situ monitoring to provide a localized index of hydrological drought in Somaliland. We find that calibrating a lumped groundwater model with a short time series of high-frequency groundwater level observations substantially improves the quantification of local water availability when compared to satellite-based indices over the same validation period. By varying the calibration length between 1-30 weeks, we find that data collection beyond 5 weeks adds little to model calibration at all three wells. This suggests that a short monitoring campaign is suitable to improve estimations of local water availability during drought, and provide superior performance compared to regional-scale satellite-based indicators. A short calibration period has practical advantages, as it allows for the relocation of sensors and rapid characterization of a large number of wells. A monitoring system with this contextualized, local information can support earlier financing and better targeting of early actions than regional DEWSs.

1 Introduction

Drought-prone regions host many of the world's least developed countries, which are experiencing increasing drought risk as a result of population pressures and increasing drought frequencies (UNDRR, 2015). For example, estimated fatalities from Somalia's 2011 drought exceeded 250,000, and a further drought in 2017 required humanitarian assistance for 6 million people (FAO 2018, FAO, 2019). Drought Early Warning Systems (DEWSs) aim to monitor and forecast drought risk, enabling early interventions that mitigate the most severe socio-economic impacts. To formulate this risk, DEWSs require evidence of drought intensity and community exposure collected by monitoring systems (UNDRR, 2015).

1.1. Current Drought Monitoring Methods for Early Warning

A range of regional-scale, satellite-based indicators are used to monitor physical drought development. The Standardized Precipitation Index (SPI) is a popular indicator for monitoring meteorological drought (McKee et al., 1993; Van Loon, 2015). The SPI indicates rainfall anomaly compared to the long-term average for that chosen time period (Sheffield et al., 2014). For agricultural drought (Van Loon, 2015), satellite-based indicators are used such as soil moisture and the Normalized Difference Vegetation Index (NDVI; Liang et al., 1994; NASA Worldview, 2022; Tarpley et al., 1984). These indicate available soil moisture for vegetation growth, which in turn indicates crop failure in areas where agriculture is non-irrigated (Brown, 2014; FEWS NET, 2021; FSNAU, 2021; Sheffield et al., 2014). However, in most arid zones during late dry seasons, water availability for human consumption depends on groundwater supply. As such, these surface indicators are not ideal for assessing hydrological droughts – the most intense form of drought that causes water shortages (Tallaksen and Van Lanen, 2004; Van Loon, 2015). Nevertheless, these same satellite-based indicators of meteorological and agricultural drought are used by DEWSs to infer the spatial intensity of hydrological drought by proxy because of a paucity of direct groundwater observations (Brown, 2014; FSNAU, 2021; FEWS NET, 2021; Kalisa et al., 2018; Sheffield et al., 2014; UCSB, 2021).

In practice, these indicators show abnormally large declines during the early stages of drought, and thus provide some evidence to trigger a national or regional early warning at a good lead-time ahead of the highest intensity phase of drought. However, despite useful lead-times, the spatial accuracy of these indicators is low due to the coarse resolution and measurement uncertainty of the satellite-data used as inputs (FSNAU, 2021; Sheffield et al., 2014; Karnieli et al., 2010; Sheffield et al., 2014). Furthermore, the extent to which seasonal changes in these indicators reflect actual underlying groundwater levels is unknown – aquifer recharge and well recovery depends heavily on drainage basin characteristics and human activity. As a result, these coarse physical drought indicators are used by practitioners with caution when determining which communities are most locally exposed to hydrological drought (Karnieli et al., 2010, Okpara et al., 2017).

During drought development, these physical indicators are viewed alongside seasonal climate forecasts from international organizations such as the GHACOF (Greater Horn of Africa Climate Outlook Forum), the Famine Early Warning Systems Network (FEWS NET), the National Oceanic and Atmospheric Administration (NOAA) and the UK Met Office, which give a low-certainty prediction of how the drought may evolve in future months (Brown, 2014; FEWS NET, 2021; FAO, 2021; Dinku et al., 2018; Mwangi et al., 2014). For shorter-range forecasts, the popular United States Geological Survey's Early Warning Explorer (USGS EWX) tool provides open access to the latest 15-day pentadal rainfall forecasts (UCSB, 2021). Meteorological forecasts are also compromised by a low spatial resolution and high uncertainty, particularly at longer lead-times. Furthermore, the scarcity of national hydrological monitoring programs in Sub-Saharan Africa prevents national agencies from augmenting these forecasts with local data (Brown et al., 2014; Stephens et al., 2016). Therefore, combining low resolution indicators of physical drought intensity with these forecasts results in high uncertainty about current and future drought exposure at the local scale (Boluwade, 2020; Dinku et al., 2018).

As a result of these limitations, drought managers, including national agencies and international NGOs, depend on national socio-economic data to spatially monitor drought exposure through evidence of drought impacts (FAO, 2018; FSNAU, 2021). These data are the primary source of information used to plan and finance early interventions with prioritized communities (Brown, 2014; Buchanan-Smith and McCelvey, 2018; FSNAU, 2021; Stephens et al., 2016). In Somalia and Somaliland, this information is made available in real-time by the United Nations Food and Agriculture Organization's Food Security and Nutrition Analysis Unit's (UN FAO FSNAU) Early Warning Early Action dashboard (FSNAU, 2021). It presents monthly data on market prices, livestock prices, migration data, disease prevalence, wages and nutrition. For example, by October 2016, when the socio-economic impacts of the 2016/17 drought first became apparent, the socio-economic indicators had reached the 'alarm' phase over 200 times across all of Somalia's administrative regions, over double the previous year's level (FSNAU, 2021).

Socio-economic data is fundamental for monitoring *vulnerabilities* to drought (Brown et al., 2014; UNDRR, 2015); however, an over-dependence on socio-economic data for monitoring real-time drought *exposure* is problematic for DEWSs. Requiring signals from socio-economic drought impacts for an early warning to be triggered means that opportunities for early, lifestyle-preserving interventions have already been missed. A further limitation is the coarse spatial and temporal resolution of the socio-economic indicators, with monthly data aggregated by FAO FSNAU in Somalia for each administrative region (Brown et al., 2014; FSNAU, 2021). This has the effect of smoothing out localized drought impacts, to the extent that DEWSs have little information on relative exposure at the community level. This can lead to poorly targeted and ill-timed interventions which may fail to mitigate the onset of malnutrition, economic losses, community displacement, famine and conflict in the most exposed communities

(Brown et al., 2014; FAO, 2014; Stephens et al., 2016).

1.2. Modern Sensors for In-Situ Groundwater Monitoring

The limitations of using regional methods to monitor hydrological drought exposure illustrate the need for alternatives. Despite advice in 2003 by UN FAO that data on groundwater-level fluctuations are "essential as a basis for management" (FAO, 2003), methods to monitor drought still widely omit in-situ groundwater data (Lewis and Liljedahl, 2010). Reasons have included the high economic cost of data collection, the labor-intensive nature of monitoring, difficulties with community participation and a lack of hydrological expertise to process the data (Ajoge, 2019; Calderwood et al., 2020; Frommen et al., 2019; Pozzi, 2013).

Advances in sensing technology have reduced the cost and complexity of in-situ monitoring to a level where it can now be implemented on an unprecedented scale (Buytaert et al., 2016; Calderwood et al., 2020; Paul and Buytaert, 2018; Open Geospatial Consortium, 2021). Modern automatic sensors have lower costs, greater accuracy, higher-frequency measurements, real-time telemetry, longer battery lives and now require less labor and expertise for installation and data processing (Calderwood et al., 2020; Paul and Buytaert, 2018). However, the long-term maintenance of in-situ sensors remains resource intensive. Therefore, in proposing a scalable method for groundwater monitoring, understanding the optimal duration of in-situ data collection for useful and cost-effective monitoring is crucial.

Here we explore whether short-term, high frequency monitoring can be used to calibrate a groundwater model sufficiently to enable accurate predictions of groundwater availability at the local scale, using a case study of three abstraction wells in Maroodi Jeex, Somaliland. The paper is structured as follows. First, we describe the groundwater model and calibration procedure. Then, by varying the calibration length between 1-30 weeks, we assess the value of additional calibration weeks for model performance. From this, a 7-week calibration is used to evaluate how effectively the model simulates observed groundwater availability compared to satellite-based proxy indicators. The calibrated wells are then simulated between 2015-20, to illustrate how the model can be used to index hydrological drought during the 2016/17 and 2019 Horn of Africa drought events. This is followed by a discussion of how this method can be scaled-up to a large number of wells, and how the information can be used in DEWSs to inform the planning of early and effective interventions during droughts.

2 Method

2.1 Modelling approach

In data-scarce regions, simple conceptual groundwater models are favored over process driven models (Beven, 2001; Mackay et al., 2014). Here, we use a modified version of the quasi-physically based AquiMod model to simulate the local water table in response to satellite derived rainfall and evapotranspiration rates

(Mackay et al., 2014). The model (fully described in Supporting Information) provides a simple and efficient method to simulate time-dependent well water levels based on a conceptual representation of groundwater systems, with a parameter set small enough to deploy automated calibration procedures at low runtimes (Beven, 2001; Mackay et al., 2014). Model inputs, comprised of daily rainfall and actual evapotranspiration values for an area surrounding the pumping well, were obtained from satellite data (Maidment et al., 2017; Sheffield et al., 2014). The model was calibrated against in-situ groundwater-level data using a Monte Carlo approach (Mackay et al., 2014; Pianosi et al., 2015).

2.2 Input data

Daily precipitation and actual evapotranspiration data for the period 2015-2020 were obtained from, respectively, TAMSAT (Tropical Applications of Meteorology using Satellite Data; Maidment et al., 2017) and AFDM (African Flood and Drought Monitor; Sheffield et al., 2014). For point-scale applications, there is higher uncertainty associated with the daily rainfall product when used at its finest 4 km spatial resolution, particularly when employing temporal downscaling from the initial 5-day cumulation product. To reduce this uncertainty, we averaged daily rainfall over a 40 km square (Maidment et al., 2017). Daily AFDM actual evapotranspiration data has a spatial resolution of 27 km. The lower spatial variability of evapotranspiration means it is associated with less uncertainty than the rainfall input (Sheffield et al., 2014). Average evapotranspiration over 54 x 54 km was calculated for model input.

Groundwater levels at 15-minute intervals were obtained using pressure transducers in three shallow, large-diameter wells in Maroodi Jeex, Somaliland. Shallow wells provide an ideal target for DEWSs because they typically run dry before deeper boreholes and thus provide an earlier drought signal in rural areas (MacAllister et al., 2020). Sensor installation took place on 21 July 2017, at sites < 10 km apart (Figure 1). The wells, although close geographically, display markedly different behavior (Figure 4b, 4c & 4d) due to differences in construction, local geology and usage. A 7-month time series of data was collected for the three wells, which reflected some of the outstanding challenges of continuous data collection in this environment including logistics, battery supply and staffing (Paul and Buytaert, 2018). The three datasets were each used for separate calibrations of the modified AquiMod model.

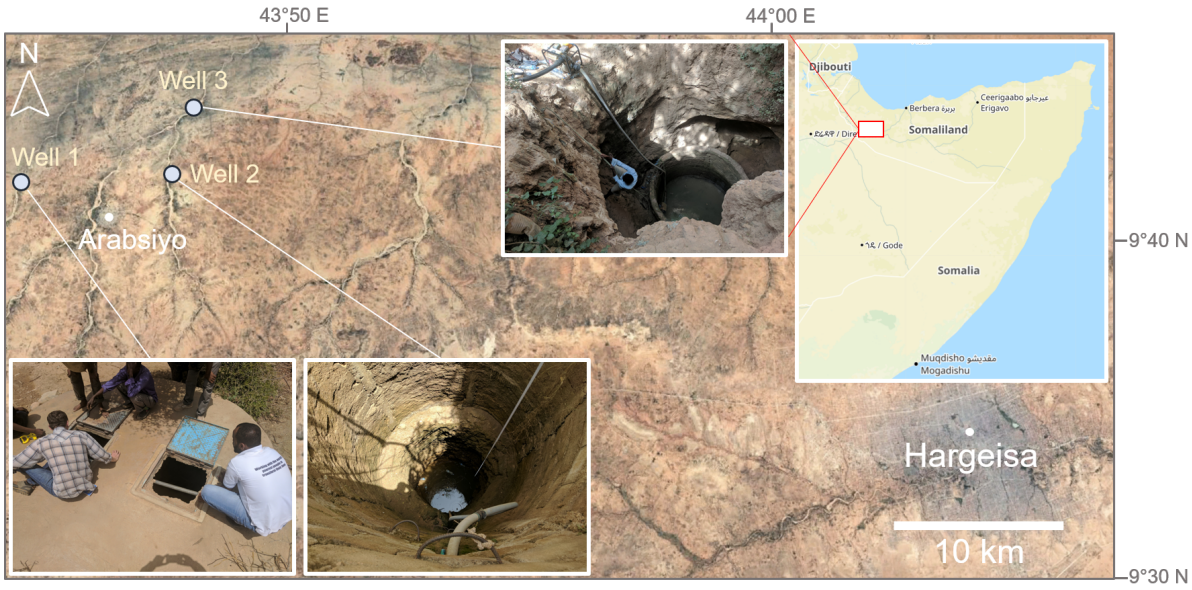

Figure 1: Location of the three shallow, large diameter wells in Maroodi Jeex, Somaliland.

2.3 Groundwater Model

We use a modified form of AquiMod (Mackay et al., 2014) to estimate aquifer recharge (R) and calculate groundwater drainage (Q_g), outputting a daily water balance for the well. The groundwater drainage component represents the loss (e.g., due to regional flow) from the aquifer, where the well is abstracting water at a rate (Q_w). The unconfined (saturated) aquifer module is represented as a single homogeneous, isotropic layer, above which is an equally homogeneous unsaturated module that is, in turn, overlain by a soil module (Figure 2). Precipitation (P) enters the top soil module following losses due to actual evapotranspiration (AE). If the soil moisture (SM) exceeds the maximum soil moisture capacity (SM_{max}), the surplus water becomes soil drainage (SD) to the unsaturated zone module. This drainage is then delayed by being distributed over time using a Weibull distribution to provide recharge (R) to the saturated module. In the saturated container, recharge from soil drainage is the sole input. The main output is the volume of groundwater drained (Q_g), which represents losses from the local groundwater system. This captures the regional flow response of the aquifer and assumes that the groundwater level drains from the system at a rate proportional to its height (H_g) above the minimum drainage level ($H_{g,min}$; Cuthbert, 2014).

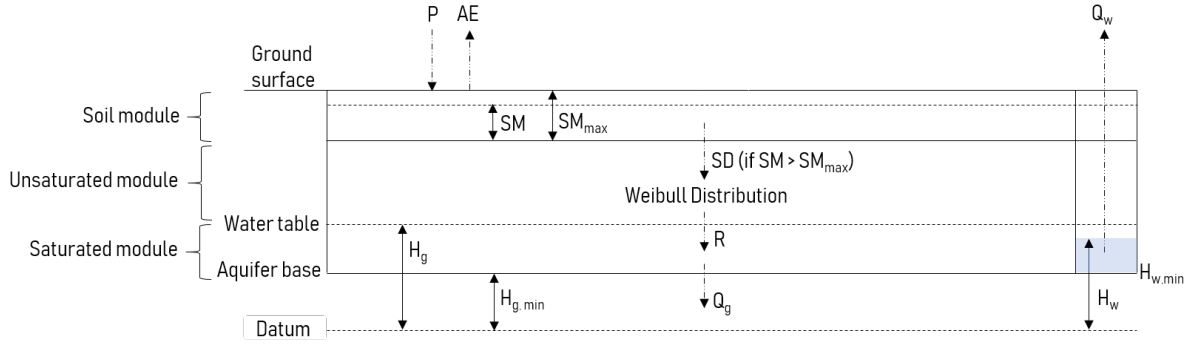

Figure 2: Modified AquiMod lumped catchment regional model for a single unconfined aquifer layer.

The model has been adapted from the single layer AquiMod model in Mackay et al. (2014) by lumping the parameters used to calculate groundwater drainage (Q_g; Figure 2). This allows the model to be reduced to a single vertical spatial dimension, where groundwater drainage (Q_g) is calculated according to the difference in the height of the groundwater level (H_g) above the base of the aquifer ($H_{g,min,}$ which is set equal to the pump inlet depth, $H_{w,min}$, as this is the 'effective' locally accessible depth of aquifer) factored by a time constant ' ' [day^{-1}]. This removes the need to represent groundwater flow using Darcy's law and thus avoids needing to determine the hydraulic conductivity at an unknown distance to an outlet on the boundary of the model. This simplification removes two additional parameters that would otherwise require calibration. The model conceptualization and the adapted equations are fully described in the Supporting Information.

Equation 1 calculates the change in groundwater level (H_g) for each timestep, by dividing the balance between the total recharge (R), drainage (Q_g) and well-abstraction (Q_w) by specific yield (S_y) and a nominal area around the well (A):

(1)

If the area is sufficiently large whereby R & Q_g » Q_w, as is common in shallow wells with low abstraction volumes, then the impacts on the regional groundwater level due to abstraction can be ignored and the recharge and groundwater drainage modeled as fluxes (r & q_g, respectively). Equation 1 is then discretised using an explicit forward difference scheme and integrated on a time step of one day, using daily recharge values obtained from the soil and unsaturated zone modules. This gives a continuous daily time-series of the unpumped groundwater level elevation (H_g) for each well site (Figure 4b, 4c, 4d; Veness et al., 2022).

2.4 Calibration Method

We calibrated the model using Monte Carlo and Global Sensitivity Analysis

(GSA) methods (Ochoa-Tocachi et al., 2018; Pianosi et al., 2015). Following sensitivity analysis, we focused on calibrating 4 sensitive parameters, while setting the remaining parameters to fixed values estimated from prior understanding of the aquifer and general hydrological systems. We sampled 10,000 combinations from a uniform distribution using Latin Hypercube Sampling (LHS; McKay et al., 1979). Input ranges were set following a manual calibration and an initial scoping study of parameter sensitivity.

In this study, the AquiMod calibration is modified so that $H_{g,i}$ is calibrated to the maximum water level in the observed data for day 'i' ($H_{w,i,max}$). In abstraction wells, pumping causes partial recovery (H_w) to the unpumped water table (H_g). This difference is at a minimum following well recovery, immediately before the onset of the following abstraction event. Therefore, calibrating $H_{g,i}$ to these daily observed peaks in groundwater level changes H_g to a simulation of 'available groundwater level' in that well. This requires an assumption that daily partial well recoveries reach a constant distance from the natural unpumped water level, which was considered appropriate based on the observed well recoveries. In datasets where $H_{g,i} - H_{w,i}$ constant, this method can be coupled to a pumping model to include the effect of variable abstraction rates on the modelled water level (see Supporting Information). For example, given the variable abstraction drawdowns and partial recoveries seen in Well 3 (Figure 4d), coupling a pumping model may improve the fit in future implementations.

2.5 Calibration Length Analysis

To assess the relationship between calibration length and model performance, the calibration period was varied at weekly intervals between 1-30 weeks. The Root Mean Square Error (RMSE) score was calculated for the full 30-week combined calibration and validation period each time (Pianosi et al., 2015). This method highlights an 'optimal' calibration period for groundwater modelling in this context, if additional weeks of in-situ observations have diminishing value in improving model performance and the challenges of monitoring outweigh the benefits. Following this, a 7-week calibration was selected as a suitable duration and used for further analysis.

The RMSE was calculated for each parameter set during the 7-week calibration period up to 6th September 2017 (4.5-week at Well 3, due to later sensor installation date), with the best scoring parameter set being the closest to zero. The best scoring set from the calibration's RMSE was then calculated in a 23-week validation (Table 1). The fit of the validations (Figure 4b, 4c and 4d) are compared to satellite-based indicators of NDVI, soil moisture and SPI-3 (Figure 4a). It is plotted alongside an uncalibrated simulation of the original AquiMod model at each well (Mackay et al., 2014), using literature derived parameter values and an understanding of the wells' locations in the alluvial, unconfined aquifer (see Supporting Information; Allen et al., 1998; Ascott et al., 2020; Domenico and Schwartz, 1990; FAO SWALIM, 2021; Jackson et al., 2016; Johnson; 1967; Lohmann, 1972; Mackay et al., 2014).

Table 1 – Parameter input ranges, calibrated parameter values and RMSE scores for the top scoring calibration sets at Wells 1, 2 and 3.

Parameter	Units	Input Range (Well 1)	Calibration (Well 1)	Input Range (Well 2)	Calibration (Well 2)	Input Range (Well 3)	Calibration (Well 3)
Sy	- day^{-1}	– 0.12 5e-4 – 1e-3	7.29e-4	– 0.01 $5e^{-5}$ – $1.5e^{-4}$	$1.02e^{-4}$	– 0.045 2e-4 – 4e-4	2.65e-4
k (Weibull)	-	- 15		- 8		- 30	
(Weibull)	-	- 30		- 30		- 30	
$H_{g\ (t=0)}$ (fixed)	m						
SM_{max} (fixed)	m						
$SM_{initial}$ (fixed)	m						
$H_{g,min}$ (fixed)	m						
RMSE (calibration)	m						
RMSE (validation)	m	-		-		-	

NDVI and Soil Moisture Active Passive (SMAP) data were downloaded at Well 2's coordinates from NASA Worldview (NASA Worldview, 2022), and daily SPI-3 values from Princeton's African Flood and Drought Monitor (Sheffield et al., 2014). NDVI is generated by the Aqua Moderate Resolution Imaging Spectroradiometer (MODIS) instrument and downloaded in 16-day intervals at a 250 m spatial resolution (NASA Worldview, 2022). The SMAP layers show a daily composite of surface soil moisture in cm^3/cm^3, calculated by the Single Channel Algorithm V-Pol for the daily half-orbit passes by the SMAP radiometer and posted to the 9-km EASE-Grid 2.0 (NASA Worldview, 2022). SPI-3 is calculated from bias-corrected Multisatellite Precipitation Analysis (TMPA) and hybrid reanalysis data (Huffman et al., 2007; Sheffield et al., 2014).

2.6 Model Simulations during 2016/17 & 2019 Droughts

Using the 7-week (4.5 week for Well 3) calibration parameters, the models were

simulated from January 2015 – December 2020 using historic rainfall and evapotranspiration as inputs (Sheffield et al., 2014; Maidment et al., 2017). The initial heads to start the model have been estimated by comparing January 2015 SPI-3/6/12 values with January 2018, for which there is corresponding observed groundwater level data, and assessing a likely groundwater level relative to the January 2018 level. The 2016/17 drought event is highlighted from the date the Somalia government declared drought (Guled, 2017) to the final observed rains of the following Gu rainy season. The 2019 drought is highlighted from the declaration date of drought emergency made by Oxfam (Barter, 2019), to the final Gu rains that year.

A critical level is defined for each well, below which the regular abstraction drawdowns observed during the dry season would not be possible. This is due to the water level falling below the pump inlet depth during abstraction drawdown, causing a 'dry pump.' A 'regular' dry season drawdown was calculated as the mean drawdown depth (m) during the final 50 observed dry season abstractions at each well. This value was then added to the pump inlet depth ($H_{w,min}$) to calculate the well's critical level.

3 Results & Discussion

3.1 Calibration Length Analysis

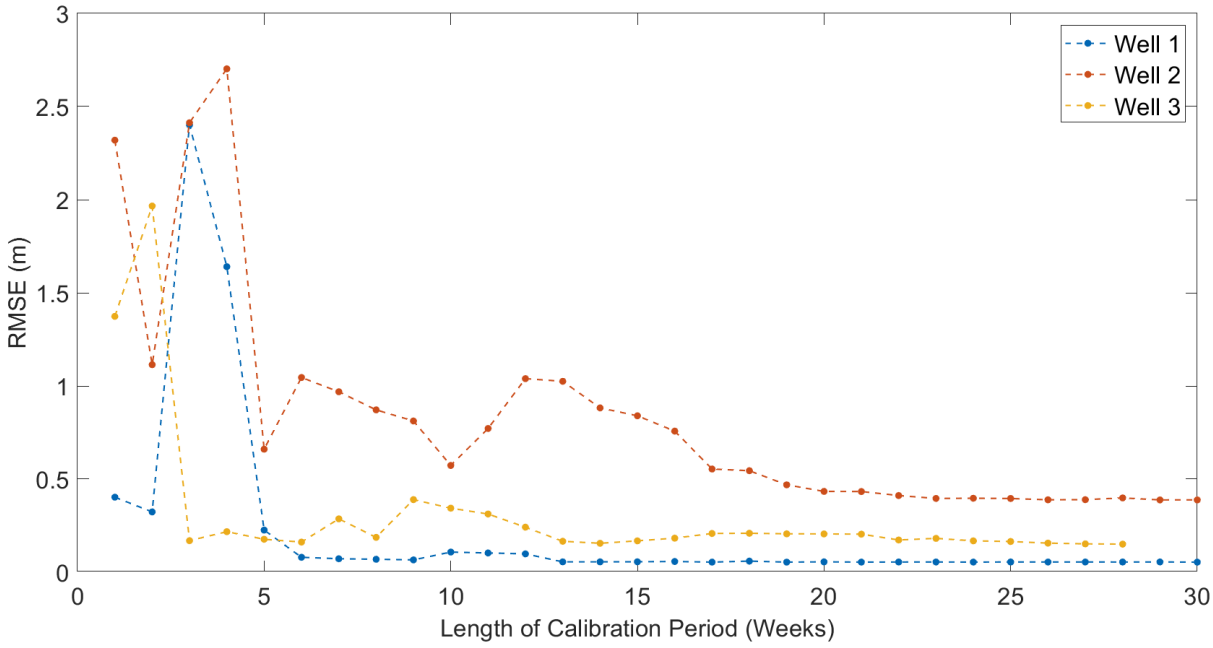

Figure 3 – RMSE for the full calibration and validation period, with calibration lengths varied at weekly intervals.

The analysis shows that there is little further improvement in calibration perfor-

mance after extending to 5 weeks (Figure 3). At this period (3 weeks at Well 3), the calibration window is long enough to include the start of the wet season, with groundwater level observations that have increased because of recharge. This causes the recharge parameters of S_y, and k to become sensitive and trained in the calibration. It is therefore essential to have a calibration period that captures observations from both the wet and dry seasons for sufficient calibration of the model. The remaining error in RMSE score at the longest calibrations will be sourced from input inaccuracies from the rainfall and evapotranspiration data, as well as modelling uncertainty with processes uncaptured by the simple, lumped parameter model (Ascott et al., 2020; Mackay et al., 2014). Following this analysis, a 7-week calibration is presented as a suitable duration that equally captures the dry and wet seasons (Figure 4b, 4c & 4d).

3.2 Model Performance

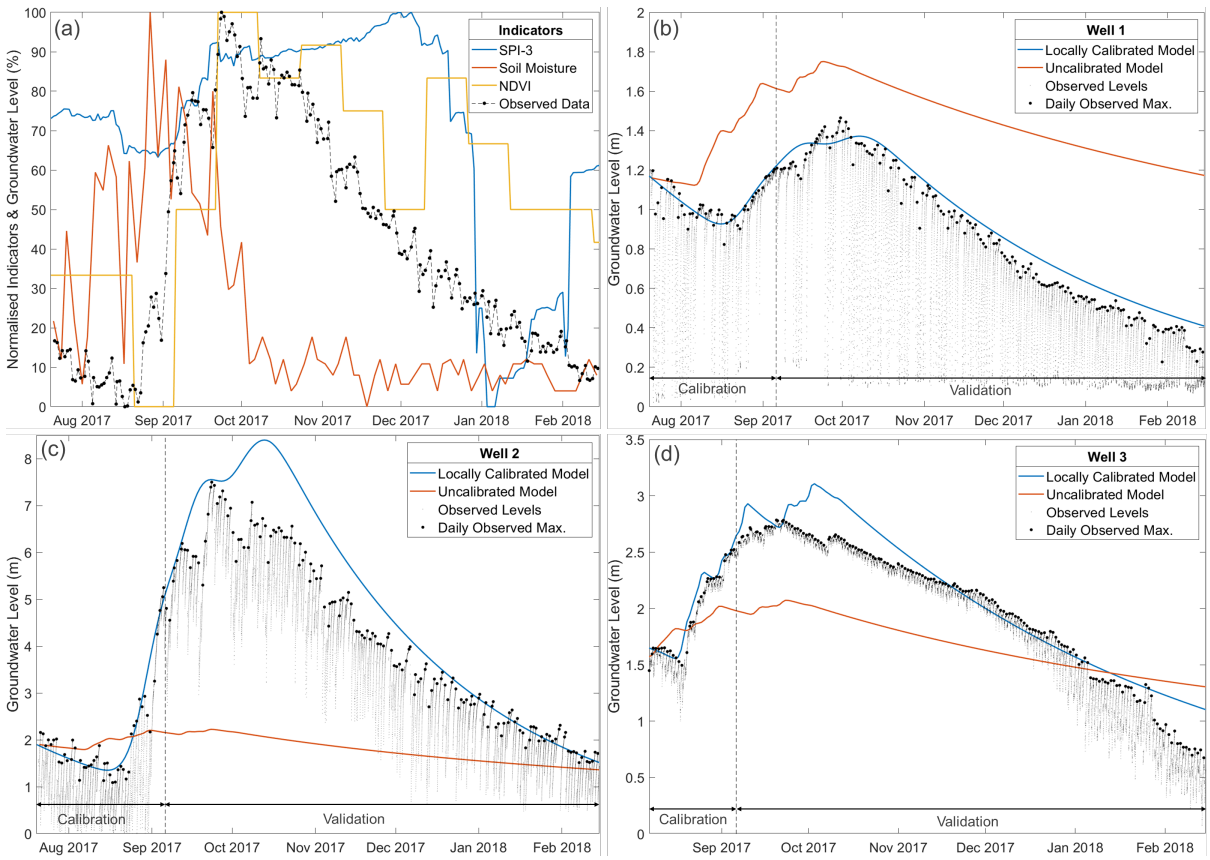

Figure 4 – (a) Normalized satellite-based proxy indicators of physical drought intensity compared to Well 2's observed daily maximum water levels. Calibrations of (b) Well 1, (c) Well 2 and (d) Well 3 are shown to compare performance with the proxy indicators and an uncalibrated AquiMod groundwater model.

Observed water levels and the corresponding calibration targets set at the daily maxima are shown for comparison of fit.

The satellite-based indicators (Figure 4a) are not suitable as proxies of local groundwater level. Soil moisture approaches its minimum months before the observed wells and remains at a flat minimum level throughout the long dry season. SPI-3 represents rainfall anomaly instead of absolute rainfall, so is unlikely to follow groundwater levels closely due to its calculation. NDVI shows the closest fit to observed groundwater levels, but it underestimates the dry season water level decline and suffers from a low temporal resolution.

Compared to the regional indicators, the calibrated model provides a substantially improved representation of observed groundwater levels (Figure 4b, 4c & 4d). The locally calibrated simulations capture the unique response of each well to recharge and dry periods, giving a reliable indication of water availability. In comparison, the poor performance of the uncalibrated groundwater model highlights the need for a local calibration, as literature-derived parameters fail to capture significant differences in well properties.

3.3 Simulating the 2017 & 2019 Droughts

To demonstrate the model's use as a localized index of groundwater availability, the calibrated wells are simulated during the two most recent droughts in Somaliland (Figure 5). These water levels are put into the context of local water availability by plotting each well's critical level, below which a full, regular abstraction drawdown would not be possible (Section 2.6).

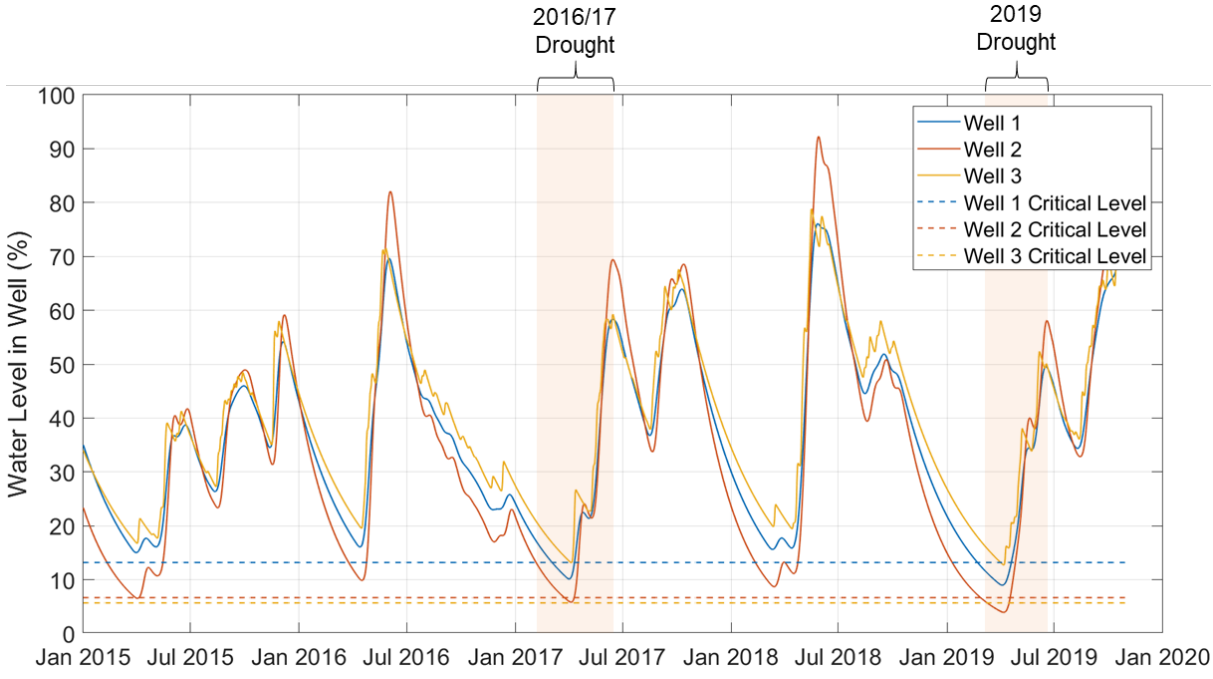

Figure 5 – 2015-20 simulations of the three wells using the 7-week calibration parameters. Water levels are normalized to the distance between the top of the well and the pump inlet depth. The two droughts are indicated from the dates that humanitarian crises were declared by the Somalia president (2017; Guled, 2017) and Oxfam (2019; Barter, 2019). The critical level is the level below which the mean observed dry-season abstraction drawdown would not be possible due to water level falling below the pump inlet.

The lowest water levels are seen during the two documented droughts (Figure 5; Barter, 2019; FEWS NET, 2021; FSNAU, 2021; Guled, 2017). Wells 1 and 2 fall below their critical level during the two droughts, indicating that regular abstraction drawdowns would have been restricted. This indicates that those wells suffered abstraction shortages during the two droughts, which may have required interventions depending on the function of the well and the socio-economic context of the community using it for water supply.

During long dry seasons where recharge is typically zero from January – early March (Figure 5, Maidment et al., 2017), this real-time visualization of water level decline enables an approximation of the lead-time before the wells reach their critical levels. However, in practice, the model inputs can simply be replaced by forecast data to simulate this lead-time for each well. On a lead-time of 1-2 weeks, datasets such as the 15-day CHIRPS-GFES pentadal rainfall forecasts can be used (UCSB, 2021). If forecasting months ahead, seasonal forecasts from GHACOF (Mwangi et al., 2014) can be used to project future water levels under different rainfall scenarios. Forecasts of water availability can therefore provide an indication of local drought exposure at the lead-time of the input forecast data.

4 Conclusions

This study finds that groundwater models with short calibrations, capturing 1-2 months of wet and dry season observations, offer substantial improvements in quantifying local groundwater availability when compared to satellite-based indicators used to infer this by proxy (Brown, 2014; FEWS NET, 2021; FSNAU, 2021; Kalisa et al., 2018; UCSB, 2021). Furthermore, by presenting water levels relative to each well's unique critical depth, the method provides a local and contextualized indicator that translates water levels to water availability (Sutanto et al., 2019).

By using modern sensors with short observation periods, the barriers to scaling-up these methods in a national-scale monitoring system are reduced. The low cost of the sensors addresses the economic hurdle of monitoring (Paul et al., 2020), and the short residence time means the sensors can be relocated to calibrate a large number of wells. The short, high frequency sensor measurements also capture abstraction behaviors, which enable the important contextualizing calculation of each well's critical water level. Although some serious challenges and ethical considerations in implementation remain, such as monitoring system governance, sensor security and community consent to participation (Buytaert

et al., 2014; Paul and Buytaert, 2018), this study highlights the renewed technical feasibility of large-scale groundwater monitoring for hydrological drought exposure.

For DEWSs, maps of real-time and forecasted water levels can be presented for the monitored wells relative to their critical depths. This enables stakeholders to compare spatial drought intensity and exposure between regions, whilst also having detailed water availability information at the local community scale. Stakeholders can then view this information alongside vulnerability data to designate interventions to communities in proportion of overall drought risk (UNDRR, 2015). These interventions commonly include provision of emergency water supplies, other lifestyle-sustaining supplies and cash transfers (Brown et al., 2014, Stephens et al., 2016). Furthermore, with forecast-based financing systems in need of more evidence to confidently trigger earlier anticipatory financing release (Stephens et al., 2016), maps of spatial drought exposure and intensity can be used to trigger the release of financing. A recent growth in parametric insurance policies for drought, seeking to payout ahead of peak impacts based on hydrological parameter thresholds being exceeded, also suggests demand for groundwater availability as a more accurate parameter to index these policies (Okpara et al., 2017).

The methodology outlined in this report is deliberately parsimonious, and it aims to serve as a demonstration of technical feasibility upon which greater complexity can later be introduced. There are considerable limitations in these methods from a traditional hydrological modelling perspective, from input uncertainties to the lumping of model parameters and the use of empirical 'critical level' calculations (Mackay et al., 2014; Maidment et al., 2017; Sheffield et al., 2014). However, groundwater modelling in a data-scarce region is intrinsically bound to modelling limitations that cannot be resolved without collecting extensive field-data, and this is simply not a feasible requirement across a monitoring network in this context (Beven, 2001). That said, data-scarce, drought-prone regions such as Somalia and Somaliland can benefit the most from groundwater models for drought modelling, forecasting and early warning. Therefore, we have proposed a viable method of generating a useful, localized groundwater availability index for DEWSs, that remains mindful of the fundamental requirement of a groundwater monitoring solution to be technically and practically feasible.

Acknowledgements

This research is funded by the UK Natural Environment Research Council [NE/S007415/1] and project partners Concern Worldwide UK, whose contribution is funded by UK AID (FCDO) and the Building Resilient Communities in Somalia (BRCiS) consortium. The authors would like to thank Paz Lopez-Rey, Kenneth Oyik, John Heelham, Dustin Caniglia, Khaled Esse Haibe and Haron Emukele for their support with fieldwork. Thanks also to Imperial College London's Grantham Institute for their support through the doctoral training program. Simon Moulds acknowledges the support of the European

Union's Horizon 2020 Research and Innovation Programme under grant agreement No.776691.

Data Availability Statement

The input data and model implementation are available online (https://github.com/veness37/ImperialWRR).

References

Ajoge, D.O. (2019) Using citizen science in monitoring groundwater levels to improve local groundwater governance, West coast, South Africa. *University of Western Cape Magister Scientiae MSc (Environ & Water Science)*, 27.

Ascott, M.J., Macdonald, D.M.J., Black, E., Verhoef, A., Nakohoun, P., Tirogo, J., Sandwidi, W.J.P., Bliefernicht, J., Sorensen, J.P.R. and Bossa, A.Y. (2020) In Situ Observations and Lumped Parameter Model Reconstructions Reveal Intra-Annual to Multidecadal Variability in Groundwater Levels in Sub-Saharan Africa. *Water Resources Research*, 56(12).

Barter, D (2019). Poor rains, persisting drought deepens crisis in Somalia and Somaliland. *Oxfam in Horn, East and Central Africa.* Available from: https://heca.oxfam.org/latest/press-release/poor-rains-persisting-drought-deepens-crisis-somalia-and-somaliland [Accessed 7 Feb. 2022].

Beven, K. (2001) How far can we go in distributed hydrological modelling? *Hydrology and Earth System Sciences*, 5(1), 1–12.

Boluwade, A. (2020) Remote sensed-based rainfall estimations over the East and West Africa regions for disaster risk management. *ISPRS Journal of Photogrammetry and Remote Sensing*, 167, 305–320.

Brown, S. (2014) Science for Humanitarian Emergencies and Resilience (SHEAR) scoping study: Annex 3 - Early warning system and risk assessment case studies. *SHEAR Technical Report.*

Buchanan-Smith, M. & McCelvey, P. (2018) A review of community-centred early warning early action systems. *Concern Worldwide Technical Report.* Available from: https://admin.concern.net/sites/default/files/media/migrated/community_centered_early_warnir [Accessed 18 August 2020].

Buytaert, W., Dewulf, A., De Bièvre, B., Clark, J. & Hannah, D. M. (2016) Citizen science for water resources management: toward polycentric monitoring and governance? *J Water Resour Plan Manage,* 142:01816002.

Buytaert, W., Zulkafli, Z., Grainger, S., Acosta, L., Tilashwork, A. C., Bastiaensen, J., De Bievre, B., Bhusal, J., Clark, J., Dewulf, A., Foggin, M., Hannah, D. M., Hergarten, C., Isaeva, A., Karpouzoglou, T., Pandeya, B., Paudel, D., Sharma, K., Steenhuis, T., Tilahun, S., Van Hecken, G. & Zhumanova, M. (2014) Citizen science in hydrology and water resources: opportunities for knowledge generation, ecosystem service management, and sustainable development. *Front. Earth Sci. Review Article.*

Calderwood, A.J., Pauloo, R.A., Yoder, A.M. & Fogg, G.E. (2020) Low-Cost, Open Source Wireless Sensor Network for Real-Time, Scalable Groundwater Monitoring. *Wate*r, 12(4), 1066.

Cuthbert, M. O. (2014) Straight thinking about groundwater recession, *Water Resour. Res.*, 50, 2407– 2424, doi:10.1002/2013WR014060.

Dinku, T., Funk, C., Peterson, P., Maidment, R., Tadesse, T., Gadain, H. & Ceccato, P. (2018) Validation of the CHIRPS satellite rainfall estimates over eastern Africa. *Quarterly Journal of the Royal Meteorological Society*, 144 (1), 292–312.

FAO (2003) Re-thinking the approach to groundwater and food security. *FAO Water Reports no. 24.* Rome.

FAO (2014) Community-based Early Warning Systems: Key Practices for DRR Implementers. *A Field Guide for Disaster Risk Reduction in Southern Africa: Key Practices for DRR Implementers.* Available from: http://www.fao.org/3/a-i3774e.pdf [Accessed 18 August 2020].

FAO (2018) Horn of Africa – Impact of Early Warning Early Action. Protecting pastoralist livelihoods ahead of drought. *FAO report.* Rome.

FAO (2019) Proactive Approaches to Drought Preparedness - Where are we now and where do we go from here? *FAO White Paper.* Rome.

FAO SWALIM (2021) FAO SWALIM: Somalia Water and Land Information Management Drought Monitoring. *FAO SWALIM: Somalia Water and Land Information Management.* Available from: http://www.faoswalim.org/water-resources/drought/drought-monitoring [Accessed 28 Mar. 2021].

FAO (2021) GIEWS - Global Information and Early Warning System. *Food and Agriculture Organization of the United Nations.* Available from: http://www.fao.org/giews/en/ [Accessed 28 Mar. 2021].

FEWS NET (2021) Famine Early Warning Systems Network. Available from: https://fews.net/. [Accessed 28 Mar. 2020].

Frommen, T., Gröschke, M. & Schneider, M. (2019) Participatory Groundwater Monitoring in India - Insights from a Case-Study in Jaipur. *Geophysical Research Abstracts,* 21, 2019–1543.

FSNAU (2021) The FSNAU Early Warning Early Action Dashboard. *FSNAU.* Available from: https://fsnau.org/special-content/fsnau-early-warning-early-action-dashboard [Accessed 28 Mar. 2021].

Guled, A. (2017) Somalia's new leader declares drought national disaster. *Associate Press.* Available at: https://apnews.com/article/97d80c7f1d0b494f9c55578a2134fa88 [Accessed 7 Feb. 2022].

Huffman, G. J., Bolvin, D. T., Nelkin, E. J., Wolff, D. B., Adler, R. F., Gu, G., Hong, Y., Bowman, K. P. & Stocker, E.F. (2007). The TRMM Multisatel-

lite Precipitation Analysis (TMPA): Quasi-Global, Multiyear, Combined-Sensor Precipitation Estimates at Fine Scales. *Journal of Hydrometeorology*, 8(1), 38–55.

Jackson, C.R., Wang, L., Pachocka, M., Mackay, J.D. & Bloomfield, J.P. (2016) Reconstruction of multi-decadal groundwater level time-series using a lumped conceptual model. *Hydrological Processes*, 30(18), 3107–3125.

Karnieli, A., Agam, N., Pinker, R.T., Anderson, M., Imhoff, M.L., Gutman, G.G., Panov, N. & Goldberg, A. (2010) Use of NDVI and Land Surface Temperature for Drought Assessment: Merits and Limitations. *Journal of Climate.* 23(3), 618–633.

Lewis, J. & Liljedahl, B. (2010) Groundwater surveys in Developing Regions. *Air, Soil and Water Research*, 3, p.ASWR.S6053

Liang, X., Lettenmaier, D. P., Wood, E. F., & Burges, S. J. (1994) A simple hydrologically based model of land surface water and energy fluxes for general circulation models, *J. Geophys. Res.*, 99(D7), 14415–14428

MacAllister, D.J., MacDonald, A.M., Kebede, S., Godfrey, S. & Calow, R. (2020). Comparative performance of rural water supplies during drought. *Nature Communications,* 11(1), 1099.

Mackay, J. D., Jackson, C. R. & Wang, L. (2014) A lumped conceptual model to simulate groundwater level time-series. *Environmental Modelling & Software*, 61, 229.

Maidment, R. I., Grimes, D., Black, E., Tarnavsky, E., Young, M., Greatrex, H., Allan, R. P., Stein, T., Nkonde, E., Senkunda, S. & Alcántara, E. M. U. (2017) A new, long-term daily satellite-based rainfall dataset for operational monitoring in Africa. *Scientific Data.* 4(170063), 170082.

NASA Worldview (2022). EOSDIS Worldview. Available from: https://worldview.earthdata.nasa.gov/?v=43.6 [Accessed 3 Feb. 2022].

Ochoa-Tocachi, B. F., Alemie, T. C., Guzman, C. D., Tilahun, S. A., Zimale, F. A., Buytaert, W. & Steenhuis, T. S. (2018) Sensitivity Analysis of the Parameter-Efficient Distributed (PED) Model for Discharge and Sediment Concentration Estimation in Degraded Humid Landscapes. *Land Degradation and Development.* 30(2), 151-165.

Okpara, J.N., Afiesimama, E.A., Anuforom, A.C., Owino, A.& Ogunjobi, K.O. (2017) The applicability of Standardized Precipitation Index: drought characterization for early warning system and weather index insurance in West Africa. *Natural Hazards*, 89(2), 555–583

Paul, J. D. & Buytaert, W. (2018) Citizen Science and Low-Cost Sensors for Integrated Water Resources Management. *Advances in Chemical Pollution, Environmental Management and Protection*, 3, 1-33.

Paul, J.D., Buytaert, W. & Sah, N. (2020) A Technical Evaluation of Lidar-Based Measurement of River Water Levels. *Water Resources Research*, 56(4).

Pianosi, F., Sarrazin, F. & Wagener, T. (2015) A Matlab toolbox for Global Sensitivity Analysis. *Environmental Modelling & Software*, 70, 80-85.

Sheffield, J., Wood, E. F., Chaney, N., Guan, K., Sadri, S., Yuan, X., Olang, L., Amani, A., Ali, A., Ogallo, L. & Demuth, S. (2014) A drought monitoring and forecasting system for sub-Sahara African water resources and food security. *Bulletin of the American Meteorological Society*, 95(6), 861–882.

Stephens, E., Coughlan de Perez, E., Kruczkiewicz, A., Boyd, E. & Suarez, P. (2015) Forecast-based Action. *University of Reading, Reading, UK (2015),* 41.

Sutanto, S.J., van der Weert, M., Wanders, N., Blauhut, V. & Van Lanen, H.A.J. (2019) Moving from drought hazard to impact forecasts. *Nature Communications*, 10(1), 1–7.

Tallaksen, L. & Van Lanen, H. (2004) Hydrological drought: processes and estimation methods for streamflow and groundwater. *Developments in Water Science.* (48) 40-50. Amsterdam, the Netherlands: Elsevier Science B.V.

UCSB (2021) CHIRPS-GEFS Climate Hazards Center - UC Santa Barbara. Available from: https://chc.ucsb.edu/data/chirps-gefs [Accessed 28 Mar. 2021].

UNDRR (2015) *Sendai Framework for Disaster Risk Reduction 2015–2030.* United Nations Office for Disaster Risk Reduction. Geneva, Switzerland, 2015.

Van Loon, A., Gleeson, T., Clark, J. R. A. & van Dijk, A. I. J. M. (2016) Drought in the Anthropocene. *Nature Geoscience,* (9) 89-91.

Veness, W. A., Butler, A. P., Ochoa-Tocachi, B. F., Moulds, S., Buytaert, W. (2022) *Imperial WRR.* Github. Available from: https://github.com/veness37/ImperialWRR [Accessed 25 Feb. 2022].